Pre-print Manuscript of Article:
Bridgelall, R., Tolliver, D. D., Rahman, M. T., Daleiden, J. F., “Pavement Performance Evaluations Using Connected Vehicles,” *International Society for Asphalt Pavements 53rd Annual Petersen Asphalt Research Conference,* Jackson Hole, WY, July 21, 2016.

Pavement Performance Evaluations Using Connected Vehicles

Raj Bridgelall[1], Md Tahmidur Rahman[2], Jerome F. Daleiden[3] and Denver D. Tolliver[4]

[1] Upper Great Plains Transportation Institute, North Dakota State University, Fargo, ND, USA, raj@bridgelall.com
[2] Fugro Roadware Inc., Austin, TX, USA, trahman@fugro.com
[3] Fugro Roadware Inc., Austin, TX, USA, jdaleiden@fugro.com
[4] Upper Great Plains Transportation Institute, North Dakota State University, Fargo, ND, USA, denver.tolliver@ndsu.edu

Abstract

The ability of any nation to support economic growth and commerce relies on their capacity to preserve and to sustain the performance of pavement assets. The ever-widening funding gap to maintain pavements challenges the scaling of existing techniques to measure ride quality. The international roughness index is the primary indicator used to assess and forecast maintenance needs. Its fixed simulation procedure has the advantage of requiring relatively few traversals to produce a consistent characterization. However, the procedure also underrepresents roughness that riders experience from spatial wavelengths that fall outside of the model’s sensitivity range. This paper introduces a connected vehicle method that fuses inertial and geospatial position data from many vehicles to expose roughness experienced from all spatial wavelengths. This study produced both roughness indices simultaneously from the same inertial profiler. The statistical distribution of their ratios agreed with a classic t-distribution. The two indices collected from three different pavement sections at two different speeds exhibit a direct proportionality within a margin-of-error that diminished below 2% as the extrapolated traversal volume approached 100. Practitioners are currently evaluating the connected vehicle method to implement lower-cost and more scalable alternatives to the international roughness index.

Keywords: Inertial profiler, intelligent transportation systems, probe vehicles, ride quality, smartphone

1. Introduction

Highway agencies measure ride quality to guide practices in roadway asset management. However, present methods that use specially instrumented vehicles and post processing are difficult to scale for network wide evaluations. The international roughness index (IRI) is currently the prevalent indicator of ride quality. Nearly all U.S. jurisdictions deploy laser-based inertial profilers to produce the IRI, which is a single index summary of roadway roughness [1]. The IRI is not a direct measurement of roughness. Rather, a mathematical procedure produces the IRI by operating on samples of the elevation profile. The procedure simulates the movement of a fixed quarter-car model across the elevation profile. The simulation moves the quarter-car at a precise speed of 80 km/h. Hence, the fixed model and the fixed simulation speed results in a very high consistency of the IRI values derived from each set of elevation profile data collected. However, the fixed parameters also lead to a misrepresentation of roughness that riders actually experience when traveling in real vehicles at different speeds.

The main contribution of this research is a method of measuring ride quality from connected vehicle data. Such a solution would scale to provide network wide, cost-effective, and continuous performance evaluations. The connected vehicle method directly samples the inertial response from many vehicles to produce an average characterization of the ride quality actually experienced [2]. Rather than a direct measurement from the actual vehicle, the IRI procedure uses a reference quarter-car model called the Golden Car [3]. The justification is that nearly all regular passenger and commercial motor vehicles, regardless of their size and weight, provide similar suspension responses because of design constraints to attenuate vibrations within the common range of frequencies that cause human discomfort [4]. In particular, humans are most sensitive to vibrations between 4 and 8 Hertz [5]. For example, the resonant frequency of the human spine is approximately 5 Hertz [5]. The typical suspension system attempts to attenuate vibrations in this frequency range and consequently result in a transfer function that exhibits a sprung- and unsprung-mass resonant mode near 1 and 10 Hertz, respectively [3].

Previous work [6] demonstrated that the Road Impact Factor (RIF) index derived from the fusion of connected vehicle sensor data is directly proportional to the IRI. The main benefit of a direct proportionality relationship is that agencies can easily estimate the IRI from RIF-indices measured using connected vehicle data. The prior experiments [6] emulated a connected vehicle by using an industrial grade device aboard a regular vehicle. The device produced high quality accelerometer, speed, and global positioning system (GPS) data. The RIF/IRI proportionality factor for those experiments was repeatable within a margin-of-error (in a 95% confidence interval) that was less than 4% after only six traversals. Hence, the main objective of this study is to repeat those experiments with a much lower cost inertial, speed, and GPS data logger implemented as a smartphone application (app) called PAVVET [6]. Testing with a commodity data logger will demonstrate the robustness of the method when deployed for practice using actual connected vehicles.

This paper reviews the distinguishing characteristics of the IRI and the RIF-transforms. To explore their relationships, the authors conducted experiments at different speeds and on different pavement sections to demonstrate their direct proportionality. The experiments used the PAVVET app aboard a certified and calibrated inertial profiler to collect both the IRI and RIF-indices simultaneously. The organization of this paper is as follows: the next section will review the models of the IRI and connected vehicle methods to highlight their respective similarities and differences. The third section will evaluate their proportionality relationship by conducting statistical analysis to test the convergence of the RIF/IRI ratios as a function of traversal volume. The fourth section will describe the case studies and discuss the significance of the results. The final section will summarize and conclude the study.

2. Ride Quality Characterizations

The IRI requires relatively few traversals to produce an average value with high precision because of its fixed Golden Car parameters and the precise traversal speed of 80 km h^{-1}. Conversely, the connected vehicle method encapsulates variations in actual vehicle suspension performance and speed, therefore, requiring a greater number of traversals to provide an equivalent level of precision.

2.1. The International Roughness Index

The definition of the IRI is the accumulated absolute rate difference between the sprung- and unsprung-mass motions of a Golden Car simulated to move at a fixed reference speed [7]. The notation for the IRI in this development is $I_{\bar{v}}^{L}$ and its definition is

$$I_{\bar{v}}^{L} = \frac{1}{L}\int_{0}^{L/\bar{v}} \left|\dot{z}_s(t) - \dot{z}_u(t)\right| dt \tag{1}$$

where $\dot{z}_s(t)$ and $\dot{z}_u(t)$ are the first derivatives of the Golden Car sprung- and unsprung-mass vertical motions, respectively. The segment length L is typically 152-meters (approximately 500-feet). The procedure fixes the speed $\bar{v}$ to the standard reference speed of 80 km h^{-1}. Therefore, the IRI ignores any variations in the actual vehicle speed and suspension responses. Although the fixed parameters enhances the precision of indices produced within relatively few traversals, the model cannot reflect roughness produced from spatial wavelengths that fall outside of a relatively narrow range. Consequently, the IRI does not reflect the true roughness that riders experience when traveling a segment at different speeds and in different vehicles.

2.2. The Road Impact Factor Transform

The RIF transform integrates the product of the vertical acceleration signal $g_z(t)$ and the longitudinal speed $v(t)$ such that

$$R_{\bar{v}}^{L} = \sqrt{\frac{1}{L}\int_{0}^{L/\bar{v}} \left|g_z(t)v(t)\right|^2 dt} \tag{2}$$

where the RIF-index $R_{\bar{v}}^{L}$ is the average g-force magnitude experienced per unit of distance L traveled. For an average speed $v(t) = \bar{v}$, within some speed band, the RIF-index simplifies to

$$R_{\bar{v}}^{L} = \bar{v}\sqrt{\frac{1}{L}\int_{0}^{L/\bar{v}} \left|g_z(t)\right|^2 dt} = \bar{v}\sqrt{E_{gz}^{L}} \tag{3}$$

where E_{gz}^{L} is the longitudinal energy density of the vertical acceleration signal. The inertial signal energy is in units of joules per meter (J/m) when the sensor output is in units of volts. The associated discrete time transform is

$$R_{\bar{v}}^{L} = \sqrt{\frac{1}{L}\sum_{n=0}^{N-1} \left|g_{z[n]} v_n\right|^2 \delta t} \tag{4}$$

where the discrete time samples are $t = n \times \delta t$ with sample instant n and average sampling period δt. The inverse of the sampling period is the sample rate of the inertial sensor. The total number of samples is N, therefore, for an average sample interval of δL, the segment length is $N \times \delta L$. Hence, the instantaneous speed is $v_n = \delta L_n/\delta t_n$ and the discrete time RIF transform simplifies to

$$R_{\bar{v}}^{L} = \sqrt{\frac{1}{N}\sum_{n=0}^{N-1} g_{z[n]}^{2} v_n} . \tag{5}$$

For a constant speed v_c, the RIF-index is related to the root-mean-squared (RMS) value of the vertical acceleration signal g_{rms} such that

$$R_{\bar{v}}^{L} = \sqrt{\frac{1}{N}\sum_{n=0}^{N-1} g_{z[n]}^{2} v_n} = \sqrt{v_c}\sqrt{\frac{1}{N}\sum_{n=0}^{N-1} g_{z[n]}^{2}} = g_{rms}\sqrt{v_c} . \tag{6}$$

It is evident that the RIF-index is zero when the traversal speed is zero and increases non-linearly with speed. Important work by others [8-9] attempted to relate the accelerometer signal to the IRI and they witnessed a speed dependency. However, those efforts did not provide a mathematical characterization to explain the dependency observed.

The RIF-transform (Equation 3) associates the RIF-index with any specified speed band whereas the IRI-transform specifies a precise speed of 80 km h^{-1}. Consequently, the RIF/IRI ratio is a function of the traversal speed. Therefore, agencies must standardize on the traversal speed selected for a given roadway facility when measuring the RIF-index to estimate the corresponding IRI.

2.3. The Ensemble Average RIF

The ensemble average of the RIF-indices (EAR) from N_v traversals across a path of length L is denoted $\bar{R}_{\bar{\bar{v}}}^{L}$ and it is analogous to the average IRI. The EAR-index is

$$\bar{R}_{\bar{\bar{v}}}^{L} = \frac{1}{N_v}\sum_{\rho=1}^{N_v} R_{\bar{v}}^{L}[\rho] \tag{7}$$

where $R_{\bar{v}}^{L}[\rho]$ is the RIF-index from the ρ^{th} traversal of the segment traveled at an average speed of $\bar{v}$, and $\bar{\bar{v}}$ is the batch mean speed of all traversals. In addition to compressing the inertial and position data longitudinally along the traversal direction, the EAR fuses multiple data streams within the same geospatial window of all traversals. Hence, the EAR-index represents a vertical compression of the stack of RIF-indices produced for a segment for some short time-period, for example, a few hours or a few days.

The EAR-index represents the average roughness that the typical vehicle occupant experiences when traveling the segment within a specified interval of speed or a speed band. For example, selecting data streams from vehicle traversals that are within 5 km/h of the IRI reference speed will produce an EAR-index that approximately summarizes roughness from the range of spatial wavelengths that the IRI is sensitive. However, producing the EAR-indices for the prevailing average speed of a given roadway facility type, such as the speed limit, would be more practical and meaningful. That is, the EAR-index will characterize ride quality from spatial wavelengths that induce roughness at the prevailing speeds rather than at the IRI reference speed. Therefore, monitoring the EAR-index from the same speed band consistently will reflect changes in ride quality that the average user experiences as the road deteriorates over time.

3. Statistical Analysis

Agencies may elect to measure and associate a calibrated RIF/IRI ratio for designated vehicles by producing the EAR-indices from several traversals of a roadway facility for which a recent IRI value is available. Alternatively, producing the EAR-index from a selected speed band by sampling the traversal data from many vehicles will obviate the need for calibration to account for the suspension behavior of a specific vehicle. Previous studies of the precision bounds in EAR-indices demonstrate that the margin-of-error, within a 95% confidence interval (MOE_{95}), diminishes rapidly after only several hours of data collection from the typical vehicle mix [10]. The MOE_{95} will diminish to equivalent levels of precision within fewer traversals when using the same vehicle or vehicle type. GIS platforms that implement this connected vehicle method would select similar classes of vehicles from the data stream, traveling under similar conditions of weather, regional climate, and roadway facility type to produce EAR-indices. A data filtering approach to select such subsets from the data stream will decrease the processing load and achieve higher precision characterizations within fewer traversals. This section will develop the statistical tests to demonstrate convergence of the RIF/IRI ratios to the expected values of a classical parameterized distribution.

3.1. Data Distribution

A histogram of the RIF-indices provides a non-parametric description of the spread from many vehicle traversals. Subsequently, the least squares approximation of a classic distribution that best fits the histogram provides a parametric estimate of their expected values to forecast the achievable precision. The critical chi-squared value tests a fitted distribution for candidacy [11].

3.2. Chi-squared Testing

The critical chi-squared value "χ^2 Data" is an evaluation of the statistic

$$\chi^2 = \sum_{k=1}^{n} \frac{\left(O_k - E_k\right)^2}{E_k} \tag{8}$$

where O_k are the histogram values observed in bin k and E_k are the corresponding expected values from the hypothesized distribution. The chi-squared distribution value at 5% significance (α = 5%) is the largest value expected with a probability of at most 5%. The chi-squared degrees of freedom (*df*) are one unit less than the number of histogram bins *n*, minus the two independent distribution parameters estimated, namely the amplitude and the mean. Estimation of the standard deviation is dependent on an estimation of the mean; hence, it does not count towards the *df*. Statisticians generally reject a null hypothesis that the data follow a tested distribution if the critical χ^2 value is larger than the chi-square distribution value at 5% significance, or equivalently, if the significance level calculated for the critical χ^2 value is less than 5%.

3.3. Margin-of-Error

The Student *t*-distribution is appropriate for sample sizes smaller than 30, and it approaches the Gaussian distribution for larger sample sizes [11]. The interval $\Delta R_{1-\alpha}^{L}$ is the margin-of-error within a (1-α)% confidence interval [12] such that

$$\Delta R_{1-\alpha}^{L} = \pm \frac{\sigma_R^L \times t_{1-\alpha/2,df}}{\sqrt{N_v}} \tag{9}$$

where $t_{1-\alpha/2,df}$ is the *t*-score at (1-α) probability for a normalized cumulative *t*-distribution of *df* degrees of freedom. The standard deviation of the RIF-index is denoted σ_R^L. The ratio of $\Delta R_{1-\alpha}^{L}$ to the EAR-index $\bar{R}_{\bar{\bar{v}}}^{L}$ is a proportional measure of the data spread as a percentage. For this study, $MOE_{0.95}$ (%) indicates that 95% of the data points are likely to be within that percentage of the EAR-index.

4. Results and Discussions

This section describes the case studies conducted, the method of data processing, and the results obtained from the field experiments. The final section tests the distribution of the RIF/IRI ratios against the classical parameterized *t*-distribution to demonstrate convergence with their expected values.

4.1. The Case Study Setting

The three pavement sections analyzed are along the frontage road sections of Texas State Highway 130, which is about 20 miles northeast of Austin, Texas. Each test site is a 210-meter section of asphalt pavement. The inertial profiler traversed each segment at approximately 72 km h^{-1} (45 MPH) and 97 km h^{-1} (60 MPH) to observe any differences in the roughness indices produced.

4.2. The IRI Data Collection and Processing

The authors used a calibrated and certified Ames Engineering Model 8300 inertial profiler. The host vehicle is a Ford E150 XLT Wagon. Resource constraints limited the number of traversals to 8 or 9 per test site. The authors subsequently used the ProVAL software to process the elevation profile samples to produce the mean IRI from the left wheel path (LWP) and right wheel path (RWP) height sensors [13].

4.3. The RIF Data Collection and Processing

The PAVVET data logger produced samples of the tri-axial acceleration, orientation, speed, time, and geospatial position coordinates from the smartphone's integrated sensors. The mounted orientation for the smartphone was vertical so that the operator could verify its operation and initiate data logging by tapping the screen. Post processing produced the resultant vertical acceleration and the corresponding RIF-index [14]. A 21-tap finite impulse response (FIR) lowpass filter with cutoff frequency of 20 Hz [15] adequately removed the noise and isolated the quarter-car sprung- and unsprung-mass modes needed to produce the RIF-indices. The RIF-transform also removes any offset in the resultant vertical acceleration to ignore static g-forces from the earth's gravity.

The maximum update rate achieved for the inertial sensors of the smartphone was approximately 93 Hz. Previous studies recommended that agencies standardize the inertial sample rate and the sensor mount apparatus to improve the precision of measurements with fewer traversal samples [15]. The data processing algorithm interpolated the distance between inertial samples by using the instantaneous speed and sample time increments. The update rate achievable from the integrated GPS receiver of the smartphone was 1 Hz. Hence, the GPS output provided a course geospatial position estimate of the path origin.

4.4. Experimental Results

Table 1 summarizes the data from the traversals of the three test sites at two speeds. The second column lists the number of traversals for each of the three test sites, and at each of the two average speeds. The third and fourth columns list the associated EAR-indices and margins-of-error, respectively. The fifth and sixth columns list the corresponding IRI and its associated margins-of-error, respectively. The last column lists the EAR/IRI ratios. As expected, the EAR-indices and the IRI for each traversal speed agree in their relative change across test sites (Figure 1a). The EAR/IRI ratios are consistent across test sites (Figure 1b).

Table 1. Summary of traversal parameters.

Site	N_v	$\overline{R}_{72}^{210}$ (g/m)	$MOE_{95(EAR)}$ (%)	I_{72}^{210} (m/km)	$MOE_{95(IRI)}$ (%)	RIF/IRI
1	7	0.225	9.5%	1.474	2.4%	0.15
2	8	0.177	13.6%	0.846	2.3%	0.21
3	8	0.168	7.4%	0.969	2.0%	0.17

Site	N_v	$\overline{R}_{97}^{210}$	$MOE_{95(EAR)}$	I_{97}^{210}	$MOE_{95(IRI)}$	RIF/IRI
1	8	0.275	9.5%	1.540	7.2%	0.18
2	9	0.202	14.2%	0.930	18.4%	0.22
3	9	0.208	7.2%	0.939	3.1%	0.31
Mean			**10.2%**		**5.9%**	

Differences in the EAR/IRI ratios arise from differences in the spatial wavelength composition of the pavements where the RIF and the IRI exhibit different sensitivities. The plots in Figure 1a show the EAR-index in units of g-force/meter (g/m) on the left axis, and the IRI in units of m/km on the right axis because of their different scales. As Equation (3) posited, the higher speed traversals produced larger EAR-indices. As anticipated, the IRI is relatively unchanged with traversal speeds because the inertial profiler maintains a fixed sample interval, and the IRI procedure uses a precise traversal speed rather than the actual vehicle speed.

As described previously, the IRI does not reflect variations in the actual vehicle speed and suspension response whereas the RIF-indices do. Hence, with only 7 to 9 traversals available per test site, the MOE_{95} for the RIF-indices were generally greater than the corresponding values for the IRI. The average MOE_{95} for the RIF-indices and the IRI was approximately 10% and 6%, respectively. This similarity in results indicates the potential for the RIF-indices to approach the precision of the IRI procedure within relatively few additional traversals.

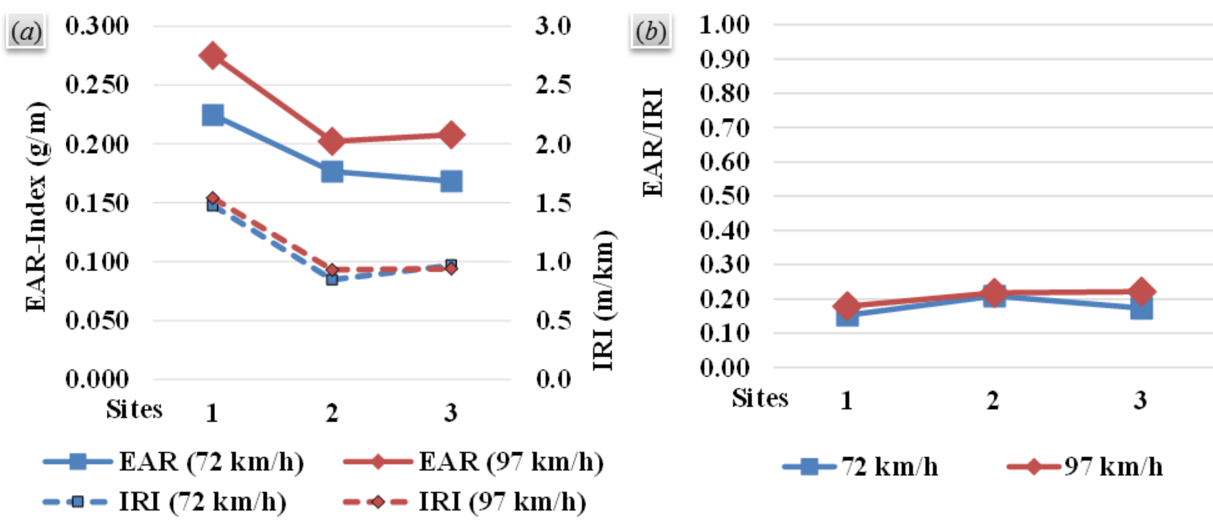

Figure 1. a) Relative change in the a) roughness indices and b) their ratios across test sites.

4.5. Convergence of RIF/IRI Proportionality

As shown in Figure 2, the histograms of the RIF/IRI ratios at two different speeds demonstrate agreement with the well-established *t*-distribution that is appropriate for data sets smaller than 30 samples.

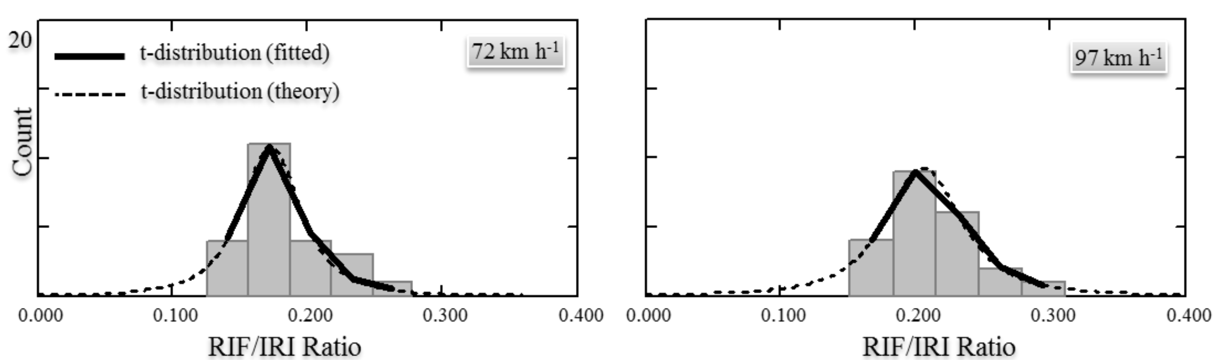

Figure 2. Distribution of RIF/IRI ratios at each traversal speed.

The law of large numbers in probability theory dictates that the average value from many trials will converge to the expected value [12]. Therefore, the RIF/IRI proportionality must converge to a mean value with increasing levels of precision as the traversal volumes from connected vehicles increase beyond 30. This guaranteed convergence in connected vehicle environments obviates the need to calibrate the RIF/IRI ratio for individual vehicles.

The critical chi-squared values calculated from Equation 8 are at 23.0% and 97.4% significance for the 72 km h^{-1} and 92 km h^{-1} traversals, respectively. These significance levels are much greater than 5%. Therefore, the chi-squared tests cannot reject a hypothesis that the distribution of the RIF/IRI ratios follows the *t*-distribution. Even with 22 to 23 samples, the MOE_{95} is 8.1% and 7.2% for the 72 km h^{-1} and 92 km h^{-1} traversals, respectively. This strong agreement with the classic distribution indicates that additional vehicle traversals will further increase the precision of estimating the IRI from connected vehicle data.

The trend of increasing precision becomes clear by plotting the MOE_{95} calculated after including data from each additional traversal (Figure 3). Extrapolating the trends based on the model indicated on the plots suggests that the MOE_{95} will diminish beyond 2% as the traversal volume approaches 100. The model for these case studies has a decay exponent of nearly -1.0, which is almost twice the theoretical floor of -0.5 (the inverse square root operation) established in Equation (9), thereby, demonstrating a much faster convergence. The coefficients of determination (R^2) for the models are nearly unity, indicating a near perfect goodness-of-fit with the data.

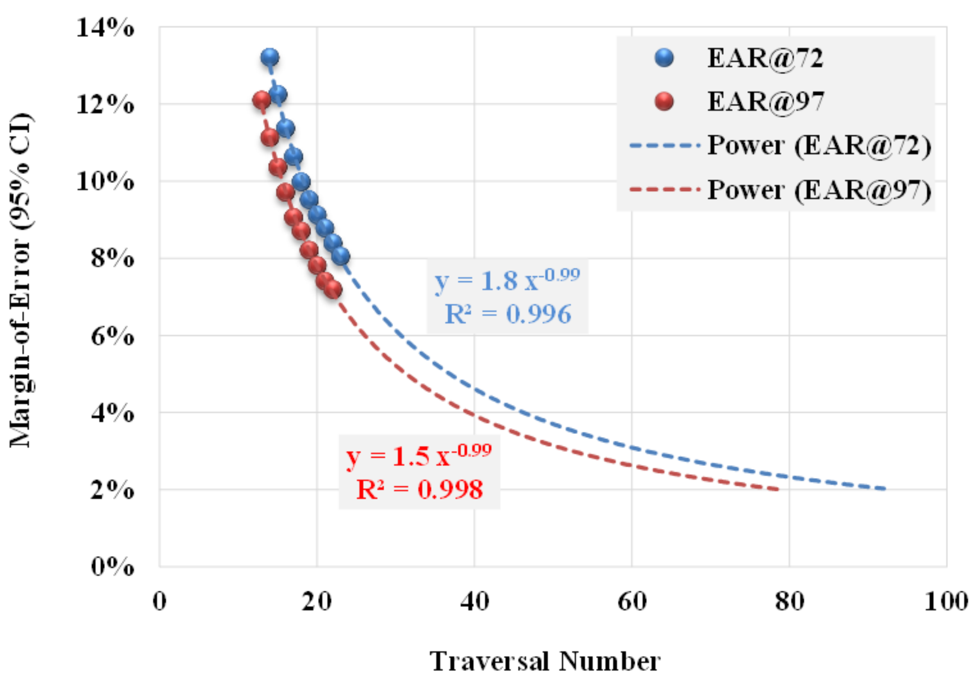

Figure 3. Margin-of-error trend for the RIF/IRI ratios.

The Annual Average Daily Traffic (AADT) volume medians are 23,000 and 82,000 passenger cars per lane for rural and urban interstate facilities, respectively [16]. Therefore, as connected vehicle environments mature, the MOE_{95} will become negligible well within one hour of data collection.

5. Summary and Conclusions

The connected vehicle method validated in this research breaks through long-standing constraints to reduce the cost, expand the reach, and increase the frequency of ride quality characterizations. The technique leverages the large volume of sensor data expected from connected vehicles to produce a consistent characterization of roughness that represents the average ride quality for any roadway facility. The case studies of this research demonstrated that the margin-of-error would diminish below 2% as the traversal volume approaches 100.

International standards for vibration safety result in a high consistency of suspension system performance to suppress roughness that produces human discomfort in a specific frequency range. Such safety standards preclude large variations in vehicle suspension responses, regardless of the vehicle size and weight; the IRI relies on this fact. Consequently, guidelines for the consistent performance of suspension systems place practically achievable bounds on the number of traversals that will produce an accurate and high-precision characterization of the true ride quality that any roadway facility provides.

The case studies conducted for this research used a certified and calibrated inertial profiler to demonstrate the direct proportionality relationship between the RIF-indices of the connected vehicle method, and the IRI. This relationship will extend investments in IRI datasets through simple scaling. Therefore, agencies have the flexibility of continuing use of the IRI while expanding applications that utilize the RIF-transform. Unlike the procedure to produce the IRI, the computational simplicity of the RIF-transform enables low-power mobile devices such as smartphones to compute them directly for real-time observation and reporting. Their computational simplicity minimizes the cost of adoption worldwide.

The connected vehicle approach addresses the IRI utility gaps by extending roughness characterizations for all roadway facility types, and at all speeds. Moreover, the average roughness indices from large traversal volumes produce a more statistically significant measure of the ride quality that users actually experience. The connected vehicle approach samples the inertial response of actual vehicles that use every roadway facility to provide a more complete characterization of the roadway network and its present ability to serve the traveling public. Furthermore, the accuracy and precision of applications that forecast pavement deterioration and localize anomalies will improve continuously with the ever-increasing volume of connected vehicle data.

Future research will examine applications of the RIF-transform to establish rules for maintenance decision support for different roadway facility types and under different environmental and usage considerations.

Acknowledgements

The University Transportation Center, a program of the United States Department of Transportation, sponsored this research through its Mountain Plains Consortium (MPC).

References

[1] *Smoothness Specifications Online - Overview of Current Practices*. The Transtec Group, Inc., March 28, 2012. SmoothPavements.com. Accessed March, 28 2015.

[2] Bridgelall, R. Connected Vehicle Approach for Pavement Roughness Evaluation. *Journal of Infrastructure Systems*, Vol. 20, No. 1, 2014, pp. 1-6.

[3] Jazar, R. N. *Vehicle Dynamics: Theory and Applications*. Springer, New York, 2008.

[4] Besinger, F. H., D. Cebon, and D. J. Cole. Force Control of a Semi-Active Damper. *Vehicle System Dynamics: International Journal of Vehicle Mechanics and Mobility*, Vol. 24, No. 9, 1995, pp. 695-723.

[5] Griffin, M. J. *Handbook of Human Vibration*. Elsevier, New York, 1990.

[6] Performance Analysis Via Vehicle Electronic Telemetry (PAVVET). Upper Great Plains Transportation Institute, December 9, 2014. www.ugpti.org/smartse. Accessed March, 28 2015.

[7] Gillespie, T. D., M. W. Sayers and C. A. V. Queiroz. *The International Road Roughness Experiment: Establishing Correlation and Calibration Standard for Measurement*. The World Bank, Washington, D.C., 1986.

[8] Dawkins, J., D. Bevly, B. Powell and R. Bishop. *Investigation of Pavement Maintenance Applications of Intellidrive*. University of Virginia, Charlottesville, Virginia, 2011.

[9] Du, Y., C. Liu, D. Wu and S. Jiang. Measurement of International Roughness Index by Using Z-Axis Accelerometers and GPS. *Mathematical Problems in Engineering*, 2014, p. 928980 (1-10).

[10] Bridgelall, R. Precision Bounds of Pavement Deterioration Forecasts from Connected Vehicles. *Journal of Infrastructure Systems*, Vol. 21, No. 1, 2015, pp. 04014033 (1-7).

[11] Agresti A., and B. Finlay. *Statistical Methods for the Social Sciences*, 4th ed., Pearson, New York, 2008.

[12] Papoulis, A. *Probalility, Random Variables, and Stochastic Processes*. McGraw-Hill, New York, 1991.

[13] Perera R. W., and G. E. Elkins. *LTPP Manual for Profile Measurements and Processing. FHWA*, U.S. Department of Transportation, 2013.

[14] Bridgelall, R. A Participatory Sensing Approach to Characterize Ride Quality. In *Proceedings of SPIE Volume 9061, Sensors and Smart Structures Technologies for Civil, Mechanical, and Aerospace Systems*, Bellingham, Washington, 2014.

[15] Bridgelall, R. Inertial Sensor Sample Rate Selection for Ride Quality Measures. *Journal of Infrastructure Systems*, Vol. 21, No. 2, 2015, pp. 04014039 (1-5).

[16] Highway Functional Classification: Concepts, Criteria and Procedures. FHWA, U.S. Department of Transportation, 2013.